Transport and Stability Study of a Fusion Power Plant Scenario

G.V. Pereverzev, E. Strumberger, S. Günter, K. Lackner

Max-Planck-Institut für Plasmaphysik, EURATOM Association, Garching, Germany

Pereverzev@ipp.mpg.de, Strumberger@ipp.mpg.de

Abstract. Various physics aspects of a fusion power plant are analyzed in this paper. An objective of this study is to verify and improve reliability of the current scaling-based predictions by a comprehensive description of plasma transport and stability. The first-principle transport model GLF has been employed for the description of the plasma core confinement. A steady-state scenario maintained by the external current drive with the bootstrap current fraction of $\geq 50\%$ is proposed and analyzed. The normalized pressure of $\beta_N = 5$ can be achieved, however, a stabilizing wall and feedback system are needed to reach high-β stable plasmas.

1. Introduction.

The EU fusion programme the "Power Plant Conceptual Study" (PPCS) [1] has been recently started. This scoping study elucidates environmental, safety and economic aspects of the future power plant although many physics issues still remain open. Namely, the physics of divertor, core confinement and stability are very essential but still not well defined elements of this scoping study. An objective of this report is to improve reliability of the scaling-based predictions by employing 1.5D plasma transport and MHD stability codes.

For the confinement analysis we used the transport code ASTRA [2] with the first-principle GLF transport model [3]. Rather moderate performance is predicted by this model for the inductive (pulsed) scenario. If no additional assumptions are involved, that results in a quite large size of the device. As an alternative to this conservative approach an advanced scenario with an internal transport barrier (ITB) has been proposed. The barrier can be maintained by an appropriately tailored external current drive at the plasma periphery. A regime with 60% of the bootstrap current and 40% of the driven current was found and investigated.

Plasma stability has been analyzed with the CASTOR_FLOW code [4]. This code is able to deal with highly reversed q-profiles that are obtained in non-inductive scenarios. Ideal stability is investigated with assumptions of ideal and resistive walls with a parameterized distance from the plasma surface. Resistive modes are also considered that can occur in ideally stable plasmas when coupled tearing modes are possible. Eventually, self-consistently calculated scenarios based on equilibrium, transport simulation and MHD stability are presented.

2. Transport model.

For transport description of the plasma core we selected the GLF transport model [3]. Credibility of this theory-based approach is supported by massive numerical and experimental efforts in the last years. Although the present-day comprehension of the core transport is relatively good there is a lack of understanding of pedestal physics. It is generally accepted that a pressure gradient in the pedestal is restricted by the ballooning limit. However, calculation of this limit is a quite subtle problem because plasma parameters (pressure, shear, safety factor, geometry) in this zone vary very rapidly, moreover, they all are strongly coupled so that occasional changing one of them can cause a long chain of related rearrangements that is very hard to trace. Instead of attempts to describe this zone by transport models and intro-

ducing uncertainties that are difficult or impossible to evaluate we shall prescribe the plasma pressure at the pedestal top and consider it as a free parameter.

As the next observation note that the density is expected to be supplied by a surface particle source (pellets or gas puffing) irrespectively of the pedestal transport. It means that prescribing the average plasma density at a given core transport one has to define the plasma density at the pedestal top, appropriately. Once the pedestal pressure is also prescribed it remains to adjust the pedestal temperature consistently that provides a complete set of boundary conditions. In this way a simulation model can be constructed that, in addition to the average plasma density, includes only one free parameter, the plasma pressure at the pedestal top.

3. Inductive (pulsed) scenarios.

3.1. Confinement properties.

In PPCS, a steady-state scenario is considered as the main operational mode although pulsed operation is also admitted as a fall-back option. This analysis will be started with a pulsed scenario because it involves a minimum of additional assumptions. Fusion powers calculated in 0D and 1.5D models for three different DEMO options [1] are compared in Table 1. The calculations (2nd line in Table 1) are performed for the fixed pedestal pressure of p_{ped} = 200 kPa that is adjusted to get close fit for the fusion powers required in PPCS. Under this assumption, the PPCS values for DEMO A and B are close to the results of transport modelling. Although numerous scalings for p_{ped} give a large scatter they typically predict a much lower value: $p_{ped} = 100$ kPa (e.g. [6]). A reduction of p_{ped} will result in a corresponding reduction of P_{Fus} that in the considered range of parameters scales approximately as $P_{Fus} \approx p_{ped}^{1.5}$. It follows that the GLF transport model predicts too low performance for the conventional pulsed scenarios. The difference is even more pronounced for DEMO C. This happens because the Model C DEMO is not compatible with the simple model discussed above. It should employ a kind of advanced scenario that will be considered below.

TABLE 1. Fusion power (GW)

Model	A	B	C
Scaling-based (0D)	5.0	3.6	3.4
Theory-based (1.5D)	4.8	3.8	1.5

In our transport model the average plasma density can be considered as an external parameter. However, the fusion power shows a very low dependence on density in the range $0.8 \leq \bar{n}_e/n_{Gr} \leq 1.4$ with a weakly pronounced maximum at $\bar{n}_e = 1.2 n_{Gr}$. The reason is that at fixed p_{ped}, increasing the plasma density results in decreasing temperature and has no effect on the plasma pressure that is mainly responsible for the fusion power. Finally, it is important to emphasize that no additional heating is assumed here. If such a heating is applied it can increase the fusion power though the effect is small because of strong confinement degradation.

3.2 Stability of plasmas with monotonic q-profile.

The ideal MHD stability of plasmas with monotonic q-profile is studied using various pressure profiles. The geometrical and physical parameters are: major radius R_0 = 8.14 m, minor radius a_0 = 2.80 m, aspect ratio A = 2.91, elongation E = 1.71, triangularity Δ = 0.35, toroidal vacuum magnetic field $B_0(R_0)$ = 5.70 T, total plasma current $I_{\rm p}$ = 21.95 MA, beta

normalized β_N = 3.59, safety factor at the magnetic axis q_a = 1.36, safety factor at the plasma boundary q_b = 4.07. The pressure, total current and bootstrap current profiles are shown in Figs 1 and 2. The pressure profile A is a peaked ASDEX Upgrade-type profile with pedestal, while the profiles B, C and D are similar to the ones given in Ref. [7,8]. As Fig. 2 illustrates, a peaked pressure profile (profile A) causes the bootstrap current to peak near the plasma centre, whereas a broad pressure profile (profile D) causes the bootstrap current to peak near the plasma edge. Due to the pedestal and the steep pressure gradient at the plasma edge of pressure profile A, the corresponding bootstrap current rises again at the plasma edge. In Fig. 3 the growth rates for ideal MHD modes are plotted as function of the toroidal mode number n. For case A the growth rate increases with rising n. This is due to the steep pressure gradient at the plasma boundary. No unstable solutions could be found for n≥3 for cases B and C. For case D the growth rate is almost constant up to n=6 and then decreases. No unstable modes could be found for n≥7.

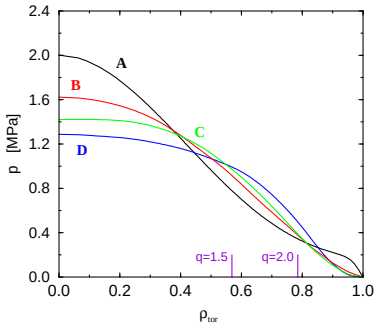

FIG. 1: Various pressure profiles named A, B , C , D .

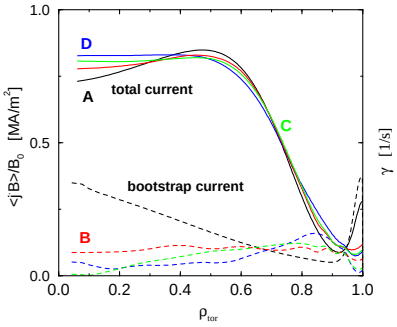

FIG. 2: Total currents and bootstrap currents.

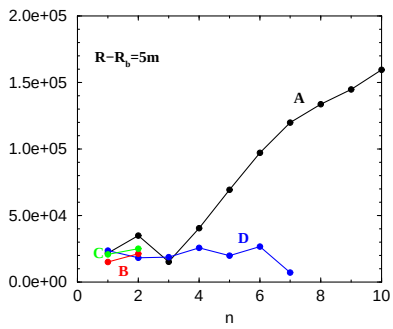

FIG. 3: Growth rates as function of n.

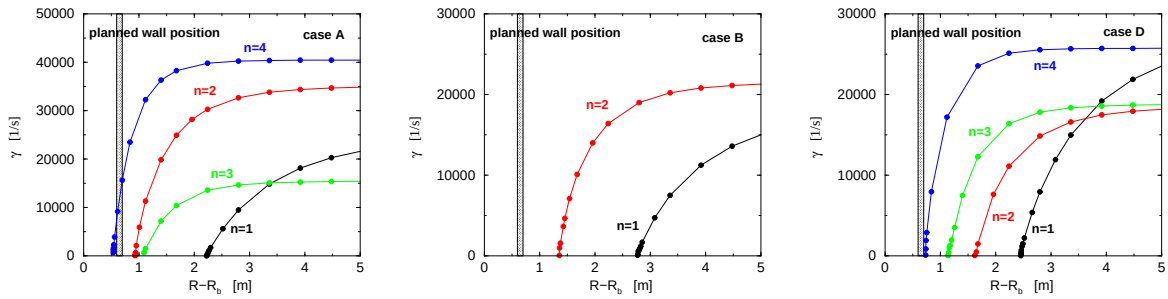

FIG. 4: Growth rates as function of the distance of the ideal wall ($R - R_b$, with R_b being the outermost radial coordinate of the plasma boundary) for cases A,B,D and n=1-4. The grey shaded area marks possible positions of an external wall in a distance between 60 and 70 cm.

In Fig. 4. the growth rates of cases A, B and D and toroidal mode numbers n=1-4 are plotted as function of the wall distance (case C is similar to case B). While modes with n≤3 are stabilized within this distance, the n=4 mode of case A stabilizes only for smaller wall distances. Furthermore, it is expected from these results that modes with n>5 can only be stabilized by an ideal wall located very closely to the plasma boundary. The high-n modes of case A are localized at the plasma edge. These modes probably give rise to edge localized modes (ELMs). In contrast to case A, the high-n modes of case D are mainly localized inside the plasma. While the considered $\beta_N = 3.59$ is already the limit for cases A and D, cases B and C would allow slightly higher values if no higher n-modes appear.

4. Advanced scenario.

An alternative to the pulsed inductive regime with a relatively poor confinement could be an advanced scenario with an internal transport barrier (ITB) where the turbulent transport is reduced or suppressed. Two essential ingredients play an important role in the formation of ITBs: low or negative magnetic shear and $E \times B$ flow shear.

4.1. Transport modelling.

In order to include ITB description in our simulation model it was assumed that the turbulent transport is suppressed in a zone of a negative magnetic shear in line with [9]. Assume now that an off-axis external current drive (e.g. due to LH or/and EC) with power deposition at the plasma periphery, $\rho_{tor} \geq 0.7$, is applied. When the driven current is high enough then a reversed shear zone can be formed as shown in Fig. 5(d,e,f). The latter is followed by a local suppression of the anomalous transport and building-up a gradient zone in temperature (Fig.5(b) and (c)). This is accompanied with a pronounced local increase of the bootstrap

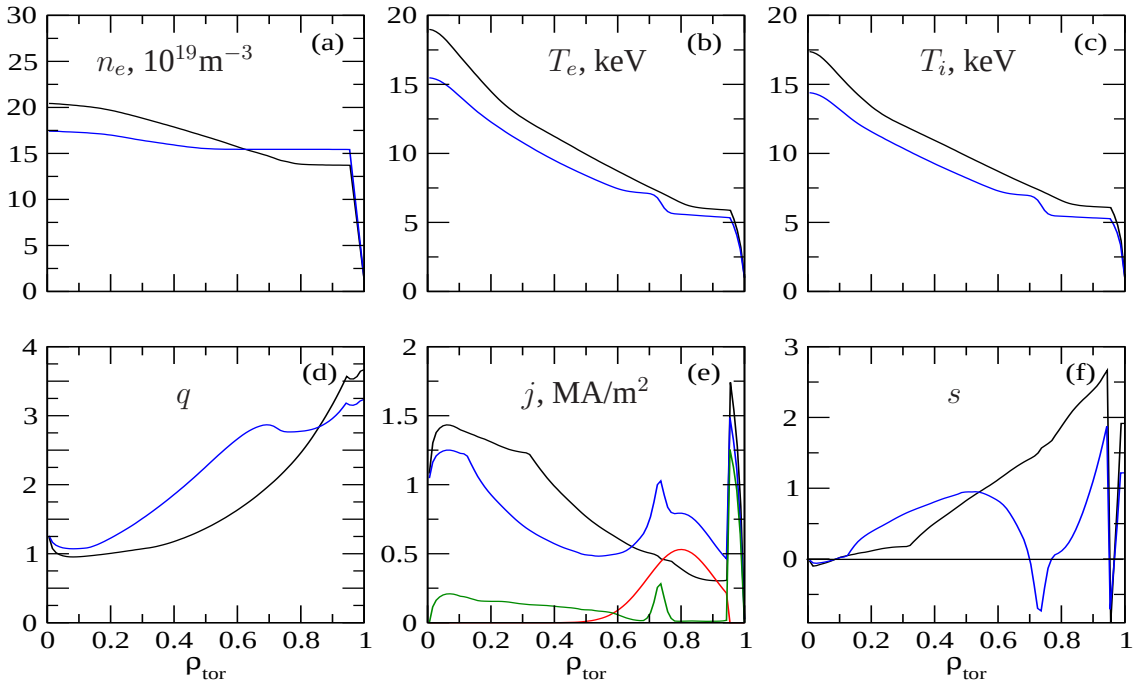

FIG. 5. ITB formation for DEMO C parameters: $R = 7.5$m, $B_T = 6$T, $I_{pl} = 20$MA. Plasma profiles are shown before (black) and shortly after (blue) applying external current drive. (a) Plasma density. (b,c) Electron and ion temperatures, respectively. (d) Safety factor. (e) The total current density, driven current (red) and the bootstrap current (green). (f) Magnetic shear.

current density. The maximum of the bootstrap current is shifted inside with respect to the maximum of non-inductively driven current. Such an alignment provides a capability of extending the negative shear region deeper into the plasma and, in turn, of broadening the ITB zone. On one hand, this process has a threshold in the external power: (i) the driven current should be large enough in order to create a seed negative shear region, (ii) this region must be sufficiently extended to result in a noticeable augmentation of the bootstrap current. On the other hand, above a certain level the secondary bootstrap current starts to grow uncontrollably.

Although this instability has a quite slow (skin-time scale ≈ 103s) growth rate its evolution can have far reaching consequences. If this instability is saturated by a mechanism similar to the "current hole" formation then it opens a route to fully non-inductive steady-state operation with a high performance. Unlike the present-day observations this regime once formed should be stable (on the diffusive time scale) because the location of ITB is defined and controlled by the external RF source. However, there is a difference to the typical current-hole formation in todays tokamaks: the ITB is started much further outside. Therefore, $q = \infty$ appears first not on the magnetic axis but around the plasma mid-radius. This corresponds to a very peculiar current profile that makes an assessment of MHD stability hardly possible.

4.2 Stability of plasmas with non-monotonic q-profile.

This equilibrium was derived by 1.5 transport modeling taking into account tokamak heating and current drive systems, as well as bootstrap current. The geometrical and physical parameters of this equilibrium are: R_0 = 8.10 m, a_0 = 2.80 m, A = 2.89, E = 1.71, Δ = 0.42, B_0 = 5.68 T, $I_{\rm p}$ = 20.08 MA, $\beta_{\rm N}$ = 1.55.

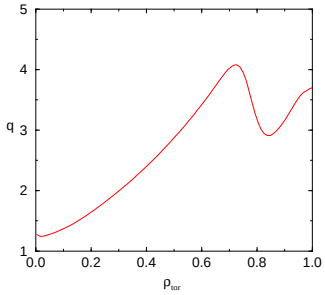

FIG. 6: Reversed q-profile.

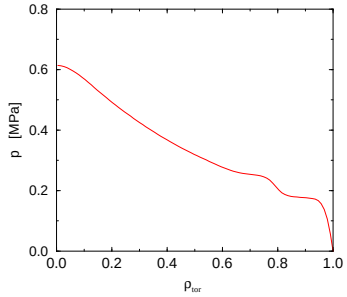

FIG. 7: Pressure profile.

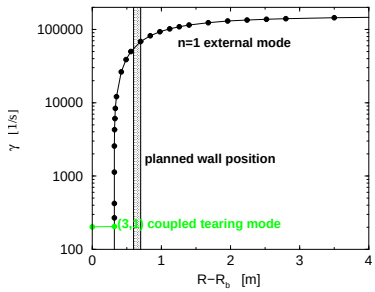

FIG. 8: Growth rate.

Already the n=1 mode can not be stabilized by an external wall within a reasonable distance (Fig. 8), because of the steep pressure gradient at the plasma edge (Fig. 7). Furthermore, when the ideal mode becomes stabilized a resistive coupled tearing mode appears. Due to the shape of the q-profile (Fig. 6) the major poloidal harmonic of the resistive mode is m=3. This mode can not be stabilized by an external wall, but also appears in case of an ideal wall located at the plasma boundary. Not shown here is the bootstrap current. Its shape fits very well the profile of the total current, but its magnitude is too small.

5. Steady-state operation.

Keeping in frames of our simulation model we will now consider another option. One can suppress the described bootstrap instability by a simple feedback algorithm

$$\frac{dP_{CD}}{dt} = \alpha_1 \left(\overline{U}_{pl} - U_0\right) + \alpha_2 \frac{d\overline{U}_{pl}}{dt}, \qquad \overline{U}_{pl}(t) = \int_{t-\Delta_t}^{t} U_{pl}(t)dt \tag{1}$$

where P_{CD} is the CD power (actuator). Averaging over the time interval $\Delta_t = 1$s is introduced because the instant value of the loop voltage $U_{pl}(t)$ can have a quite erratic behaviour. The parameter U_0 defines the fraction of residual Ohmic current. In particular, $U_0 = 0$ corresponds to fully non-inductive operation. Finally, the two parameters $\alpha_{1,2}$ are adjusted to obtain desired properties of the control. The rule (1) is effective provided that driven and

bootstrap currents are localised sufficiently close to the plasma surface where the loop voltage is measured. If the algorithm (1) is applied every 1 s it gives rather robust control of the bootstrap current fraction provided this fraction is not too high, in practice $\leq 60\%$.

Comparison of PPCS data with the transport modelling is presented table in Table 2. Despite the pedestal pressure is reduced with respect to Table 1 down to 100 kPa the fusion

TABLE 2. Advanced scenarios for DEMO-C model ($R = 7.5$m, $B_T = 6$ T).

Model	I_{pl}	P_{Fus}, GW	P_{add}, MW	n/n_G	I_{BS}/I	Q	U_0, V	p_{ped}, kPa
0D	20.1	3.41	112	1.5	0.63	30	–	–
1.5D	16	1.5	130	1.2	0.41	11.3	0.01	100
	16	2	122	1.2	0.49	16.3	0.005	100
	16	2.1	95	1	0.56	22.5	0	100

power increases. This pedestal pressure can be considered as quite plausible and results are not very far from predictions of PPCS. The only essential difference is the reduction of the total plasma current that is necessary for keeping the driven current fraction high enough.

Plasma profiles for the steady state scenario (the bottom row in Table 2) are shown in Fig. 9. Here the time averaged Ohmic current and the loop voltage are equal to zero and the feedback algorithm maintains the bootstrap current at the level of 8.9 MA. An extended zone of negative shear and improved confinement is localised around $\rho_{tor} = 0.75$ where the bootstrap

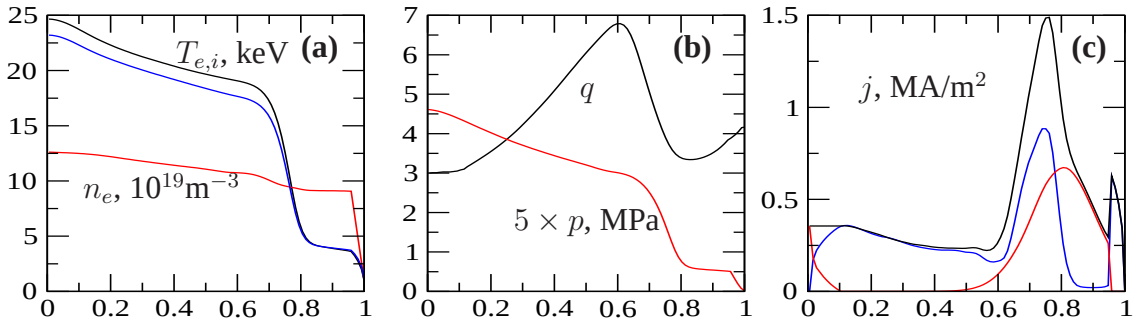

FIG. 9. Plasma profiles for a steady state scenario with the feedback control of the loop voltage. Here $R = 7.5$m, $B_T = 6$T, $I_{pl} = 16$MA. (a) Plasma density, electron and ion temperatures. (b) Safety factor q and plasma pressure p. (c) Total current (black), driven (red) and bootstrap (blue) current densities.

current has maximum. An artificial seed current is added in the vicinity of the magnetic axis. A total of 40 kA of this current is needed in order to fill the central gap in the bootstrap current. The rest of 7.1 MA with a maximum at $\rho_{tor} = 0.8.$ is assumed to be driven by an external source and is used as an actuator in the feedback scheme (1). Stability of the steady state distributions shown in Fig. 9 and and a stable route to this regime will be a subject of following studies.

6. Stability and bootstrap current of optimized scenario.

Here we use optimized profiles of the safety factor (Fig. 11), pressure and density (Fig. 10) developed for the advanced tokamak power plant ARIES AT by C.E. Kessel et al. [8].

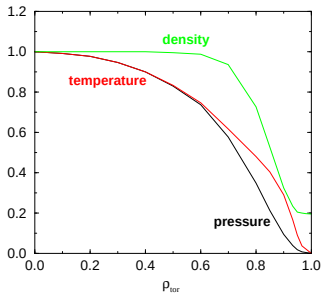

FIG. 10: p, T, n-profiles.

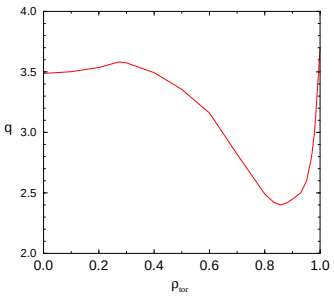

FIG. 11: q-profile.

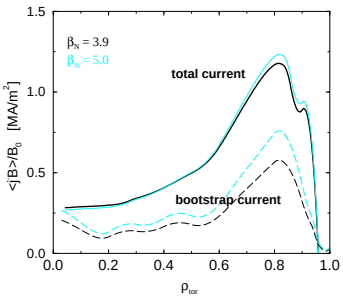

FIG. 12: Current profiles.

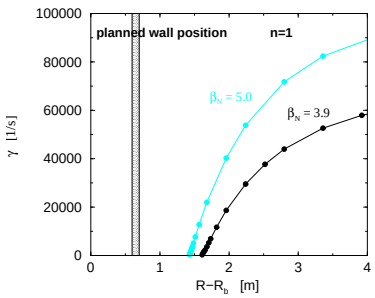

FIG. 13: Growth rates as function of the wall distance.

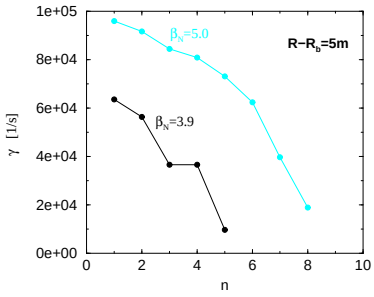

FIG. 14: Growth rates as function of n.

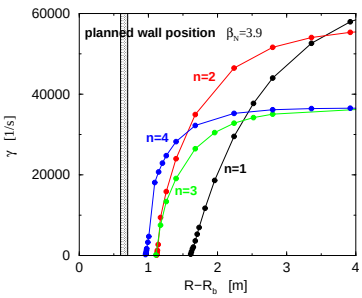

FIG. 15: Growth rates as function of the wall distance.

Using these profiles, equilibria for two β_N-values are investigated. The geometrical and physical plasma parameters are: R_0 = 8.10 m, a_0 = 2.80 m, A = 2.89, E = 1.70, Δ = 0.48, B_0 = 5.64, I_p = 24.-25 MA, β_N = 3.9 -5.0. The bootstrap current profiles align very well with the total current profiles (Fig. 12). In case of $\beta_N = 5.0$ the bootstrap current fraction exceeds 50%. The growth rates as function of the ideal wall distance and the toroidal mode number are plotted for two β_N-values in Figs 13 and 14. As expected, the growth rates increase with increasing plasma beta, whereas the stabilizing distance of the wall is reduced. For n=1-4 the growth rates as function of the wall distance are shown for β_N=3.9 in Fig. 15. Both, the growth rate and the stabilizing wall distance decrease with rising n.

7. Conclusions and outlook.

Conventional pulsed scenarios for DEMO are hardly compatible with predictions of the GLF transport model and current pedestal models. Advanced approaches are required to achieve DEMO performance goals. In this paper, a steady-state non-inductive scenario is proposed. Improved confinement is due to negative shear largely created by the bootstrap current ($\approx 55\%$) and stabilised by externally driven current. This regime has evident attraction for high-Q steady state operation. Unfortunately, it is difficult to reproduce this regime in existing tokamaks because it requires (i) high power production in the plasma core, (ii) peripheral current drive with a high power at the initial trigger phase of the process at least. Studying this opportunity could be a challenging task for ITER operation. The regime will be further optimised with respect to plasma current, density, CD power deposition profile and other parameters. MHD stability of the regime and a stable route to it still remain open issues.

Within the framework of linear MHD theory it is possible to design high-β tokamak equilibria with appropriate profile and magnitude of the bootstrap current, and desirable stability properties. The discussed optimized equilibrium is at least stable up to β_N=5, and the boot-

strap current fraction exceeds 50%. The shape of the bootstrap current is well aligned with the total current profile. Nevertheless, none of the investigated equilibria is stable without external wall. This result underlines the need of stabilization structures, that is, resistive wall plus feedback system, in order to reach stable high-β plasma equilibria. The studies of various types of equilibria further show that also modes with n>2 may play an important role. Usually, the stabilizing distance of the external wall decreases with increasing toroidal mode number. Some of the equilibria become more and more unstable with increasing toroidal mode number. This is due to their steep pressure gradient at the plasma boundary. The transport consistent equilibrium demonstrates that if an equilibrium turns out to be ideal stable, its stability behaviour with respect to resistive modes should also be investigated in detail.

In linear ideal MHD theory only equilibria with rational surfaces outside the plasma boundary (m/n> q_{b}) can be unstable with respect to external kink modes. That is, an equilibrium limited by a separatrix ($q \rightarrow \infty$) would be stable with respect to these modes. For the presented ideal MHD stability studies we used hypothetical plasma configurations with finite q-value at the plasma boundary, namely $q_{\mathrm{b}} = 3.8 - 4.2$, and plasma shapes (no separatrix) with elongation $E = 1.70 - 1.96$ and triangularity $\Delta = 0.35 - 0.57$. But, whether a plasma is stable with respect to an external kink mode, or whether this mode can be stabilized by an external wall located in a technically feasible distance, depends sensitively on the choice of these parameters. Stability computations for the same core plasma, but slightly different plasma boundaries yield different results. Therefore, more realistic computations should be performed. As a first step, free-boundary equilibria should be calculated in order to obtain profound information on the overall equilibrium. Further, in contrast to the assumptions of the used ideal MHD model, there is a smooth transition from an almost ideal core plasma to the surrounding non-conducting vacuum. In the boundary region of a real plasma the resistivity increases continously due to the decreasing temperature. And, the external wall is also resistive. For future computations we therefore suggest to take these resistivities into account and to perform the stability studies for plasma boundaries sufficiently close to the separatrix.

References

[1] EUROPEAN FUSION DEVELOPMENT AGREEMENT, A Conceptual Study of Commercial Fusion Power Plants, EFDA-RP-RE-5.0, EFDA Report, April 13th, 2005.
[2] PEREVERZEV, G.V., YUSHMANOV, P.N., ASTRA - Automated System for Transport Analysis, Report IPP 5/98, Max-Planck-Institut für Plasmaphysik, Garching, 2002.
[3] WALTZ, R.E., et al., Phys. Plasmas **4** (1997) 2482-2496.
[4] STRUMBERGER, E., et al., Nuclear Fusion **45** (2005) 1156-1167.
[5] MUKHOVATOV, V., et al., Nucl. Fusion **43** (2003) 942-948.
[6] SUGIHARA, M., et al., Plasma Phys. Control. Fusion **45** (2003) L55-L62.
[7] KESSEL, C.E., Nuclear Fusion **34** (1994) 1221-1238.
[8] KESSEL, C.E., et al., Fusion Engineering and Design **80** (2006) 63-77.
[9] TALA, T., et al., Nucl. Fusion **46** (2006) 548-561.